THERMODYNAMIC IMPACT OF MOLTEN SLAGS ON THE FORMATION BEHAVIOR OF MGO-AL_2O_3-TiO_X INCLUSION IN STEEL MELTS

Joo Hyun Park
University of Ulsan, Korea

Sang-Beom Lee
Technical Research Laboratories, Korea

Henri Gaye
Institute of Ferrous Technology, Korea

ABSTRACT

The equilibration between CaO-SiO_2-MgO-Al_2O_3-CaF_2 (-TiO_2) slag and Fe-11wt%Cr ferritic stainless steel melts was investigated at 1873 K in order to clarify the effect of Al and Ti addition as well as that of slag composition on the formation of complex oxide inclusions. The activity of oxygen from [Al]/(Al_2O_3) and that from [Si]/(SiO_2) equilibria is relatively in good agreement to each other with some scatters. The composition of the inclusions could be plotted on the computed MgO-Al_2O_3-TiO_x phase diagram. The inclusions in the steel melts equilibrated with the basic slags are located in the "spinel + liquid" region, while those in equilibrium with the less basic slags are mostly in the "liquid" single phase. However, in cases of high concentration of Ti and Al, the inclusions were found to be "spinel + liquid", even though the less basic slags are equilibrated. The spinel potential, log $(X_{MgO} \times X_{Al_2O_3}/X_{Ti_2O_3})$ *is very low and nearly constant when the activity of* Al_2O_3 *is less than that of* TiO_2 *in the slag saturated by MgO, whereas it linearly increases by increasing the log* $(a_{Al_2O_3}/a_{TiO_2})$ *at* $(X_{Al_2O_3}/X_{TiO_2}) > 1$.

INTRODUCTION

Clogging phenomena of SEN or tundish nozzle during continuous casting of Ti-stabilized stainless steels have been investigated by several researchers. Gao and Sorimachi indicated that the major materials deposited in an immersed nozzle were globular Ti oxide and alumina agglomerates, whereas TiN and Al_2O_3 were observed in molten steel (Type 409) in the tundish along with a minor amount of Ti oxides.[1] Maddalena *et al.* [2] reported that the presence of magnesium aluminate spinel in the stainless steels (Types 321 and 409) accelerates the growth of the deposits from their observation of two distinct types of TiN based deposits during analysis of clogged nozzles; pure TiN in a three dimensional array and TiN particles apparently connected via spinel phase. Recently, Nunnington and Sutcliffe observed the oxidation of TiN inclusion in type 441 stainless steel and postulated the formation of titanium oxynitride, $Ti(ON)_{ss}$ from the high mutual solid solubility of TiO and TiN in the cubic structure.[3] The effect of Al and Ti deoxidation on the formation of $CaTiO_3$-$MgAl_2O_4$ dual phase inclusion was formerly investigated by Kim *et al.*[4, 5] for types 304 and 430 stainless steels. Even though these studies described well the phenomena of the clogging and inclusions in the stainless steel industry, thermodynamic understanding for the effect of slag composition on the complex oxides in Ti-stabilized ferritic stainless steel is still insufficient.

In-depth thermodynamic and kinetic studies on the effect of slag on the formation mechanism of spinel inclusions in Ti-free 16 wt%Cr ferritic stainless steel have been investigated by Park and Kim,[6] and Okuyama *et al.* [7], respectively. In the former study, the more basic slag (CaO or MgO saturation) equilibrated with the molten steel, the more MgO-rich spinel inclusions were observed.[6] In the latter, the concentration of MgO in the inclusions increased by increasing the ratio of CaO to SiO_2 (or Al_2O_3) in the top slag and the rate determining step was proposed as a diffusion of Mg in molten steel deoxidized by Al. [7] Therefore, in the present study, based on the preceding view of thermodynamic and kinetic studies, the equilibration between CaO-SiO_2-MgO-Al_2O_3-CaF_2 (-TiO_2) slag and Ti-stabilized Fe-11 wt%Cr ferritic stainless steel melts has been investigated at 1873 K in order to clarify the effect of Al and Ti addition as well as that of slag composition on the formation of complex oxide inclusions containing Ti.

EXPERIMENTAL

Pure Fe, Cr, Si, and Mn (>99.9%) were premelted in a vacuum induction furnace to make a nominal composition of Fe-11%Cr-0.5 %Si-0.3 %Mn ferritic stainless steel. Alloys of about 730 g and the premelted CaO-SiO_2-MgO-Al_2O_3-4%CaF_2 slags (B=(%CaO+%MgO)/(%SiO_2 + %Al_2O_3)=0.9-1.7)) of 20-30 g were equilibrated in MgO crucibles at 1873 K, heated in an induction furnace. The initial contents of dissolved Al and Ti in the premelted alloy were approximately less than 25 ppm.

The stainless steel reaction chamber, which was cooled by cooling water, was initially evacuated by the mechanical rotary pump and filled by Ar gas (1.01×10^5 Pa) and followed by induction heating. The temperature was established to be 1873 K using an R-type (Pt-13 wt%Rh/Pt) thermocouple and a proportional integral differential controller. The oxygen in Ar gas was removed by passing the gas through Mg turnings heated to about 773 K, even though 99.999% purity Ar gas was used. After the steel samples were melted at 1873 K, the premelted slags were added and followed by the addition of Al less than about 200 ppm. After 3 minutes, a fixed amount of sponge Ti equivalent to about 0.3 wt% was added. All of the additives such as slags and metals were dropped through the quartz tube under an inert atmosphere. Then, the system was equilibrated during about 60 minutes,

which was determined by the preliminary equilibrium experiments. It was confirmed that the slag was saturated by MgO. After equilibrating, the power of the furnace was turned off and the crucible assembly was quenched by helium gas, which was blown from the top surface of the crucible. A schematic diagram of the experimental apparatus is shown in Figure 1.

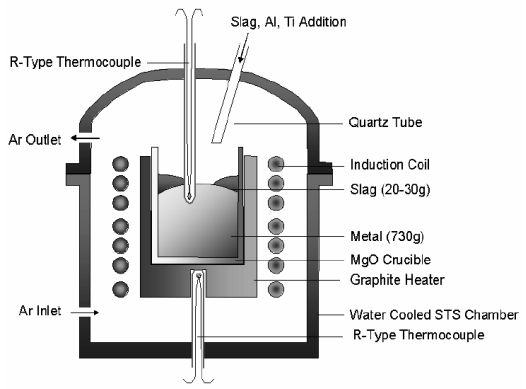

Figure 1: Schematic diagram of the experimental apparatus

The content of Cr, Si, Mn, and total Al was analyzed by an optical emission spectrometry and the content of dissolved Al, Ti, and Mg was determined by the ICP-AES. The content of O and N was analyzed by fusion and the infrared absorption method after very careful preparation through an ultrasonic cleaning. The composition of the slag was analyzed by an XRF spectroscope.

The steel samples were mounted in cold-setting resin. Next, standard grinding and polishing techniques were used, after which all samples were gold coated. Finally, the compositions of about ten inclusions per sample were determined by using a SEM and EDS. The composition of the inclusion in each sample was taken from the average value of about ten inclusions.

RESULTS AND DISCUSSION

The addition of Al into the Si deoxidized Fe-11 %Cr-0.5 %Si-0.3 %Mn steel changes the activity of oxygen in the melt, which is also affected by the equilibrium between metal and slag. The equilibrium deoxidation reaction by Al and Si is given in Equations 1 and 3, respectively [8].

$$2[\mathrm{Al}] + 3[\mathrm{O}] = (\mathrm{Al_2O_3})^{\mathrm{slag}} \tag{1}$$

$$\log K_{[1]} = \log\left[a_{\mathrm{Al_2O_3}} \Big/ a_{\mathrm{Al}}^2 \times a_{\mathrm{O}}^3\right] = 45{,}300/T - 11.62 \tag{2}$$

$$[\mathrm{Si}] + 2[\mathrm{O}] = (\mathrm{SiO_2})^{\mathrm{slag}} \tag{3}$$

$$\log K_{[3]} = \log\left[a_{\mathrm{SiO_2}} \Big/ a_{\mathrm{Si}} \times a_{\mathrm{O}}^2\right] = 24{,}600/T - 8.4 \tag{4}$$

where $K_{[n]}$ and $_{ai}$ are the equilibrium constant of Equation (n) and the activity of element *i* in the steel melt. The activity of oxygen determined by the equilibrium of [Al]/(Al_2O_3), a_O^{Al} and by [Si]/(SiO_2), a_O^{Si} can be estimated from Equations 5 and 6, respectively.

$$\log a_O^{Al} = 1/3\left(\log a_{Al_2O_3} - 2\log a_{Al} - \log K_{[1]}\right) \quad (5)$$

$$\log a_O^{Si} = 1/2\left(\log a_{SiO_2} - \log a_{Si} - \log K_{[3]}\right) \quad (6)$$

In addition, the activity coefficient of solute (M) can also be calculated by the Wagner formalism using the first- and second-order interaction parameters, which are listed in Table 1.[8]

$$\log f_M = \sum_{i=Cr,Si,Mn,Al,Ti,Mg,O}\left(e_M^i \times [\text{mass pct i}] + r_M^i \times [\text{mass pct i}]^2\right) \quad (7)$$

Where f_M, *e* and *r* is, respectively, the Henrian activity coefficient of element M, and the first-and second-order interaction parameters between each element. In Figure 2, the activities of oxygen calculated from the [Al]/(Al_2O_3) equilibrium and that from the [Si]/(SiO_2) equilibrium are plotted against the activity of oxygen from the classical Wagner formalism, where the concentration of dissolved oxygen was taken by the average of oxygen determined from [Al]/(Al_2O_3) and [Si]/(SiO_2) equilibria. Also, the activity of Al_2O_3 and SiO_2 in the slag at 1873 K was taken from the thermodynamic data reported by Ohta and Suito by assuming that the effect of about 5 wt%CaF_2 and 12 wt%TiO_2 would not seriously affect the activity coefficient of SiO_2 and Al_2O_3 [9]. The activity of oxygen from the classical Wagner formalism changes from about log a_O = -3.7 to -2.9 and the values of $a_O^{Al}$and a_O^{Si} are relatively in good correspondence to each other with some scatters.

This tendency shows quite fair accordance to the thermodynamic equilibrium of the present slag-metal system, which has been discussed by one of the authors (HRG) *et al.*[10] on the basis of thermodynamic model (IRSID slag model) and experimental data.

The composition of the inclusions is plotted on the MgO-Al_2O_3-TiO_x ternary phase diagram (Figure 3), which was computed by using FactSage™ 5.5 program with the *FACT53* and *FToxid* databases at 1873 K and p_{O_2} = 10^{-13} atm, [11] which corresponds to the average value of oxygen activity (Figure 2) based on Equations. (8) and (9).[8]

$$1/2\ O_2\ (g) = [O] \quad (8)$$

$$\log K_{[8]} = \log a_O \Big/ p_{O_2}^{1/2} = 6{,}120/T + 0.18 \quad (9)$$

In Figure 3, four solid phases such as spinel, Al_2O_3, MgO, and pseudobrookite (mainly Ti_3O_5) are in equilibrium with the liquid phase. The present phase diagram is relatively similar to those calculated by Kaufman and one of the authors (HRG) *et al.* [12, 13]. However, because of the differences not only in the oxygen potential but also in thermodynamic models used in each study, there are some differences in the phase diagrams, especially in the area of fully liquid phase. It is noticeable that the inclusions in the steel melts equilibrated with the relatively basic slags (*B* > 1.7)

Table 1: Interaction parameters used in the present study

e_i^j (r_i^j)	Cr	Si	Mn	Al	Ti	Mg	O
Al	0.030	0.056	0.035	0.043	0.016	-0.30	-1.98 (39.82)
Ti	0.029	-0.025	-0.043	0.024	0.042	-1.27*	-1.62 (-0.36)
Si	-0.021	0.10	-0.007*	0.058	-0.013*	-0.11*	-0.12
Mg	0.022	-0.096	-	-0.27	-0.64	-	560 (145,000)
O	-0.032	-0.066	-0.037	-1.17 (-0.010)	-0.54 (0.039)	-370 (5,900)	-0.17

* Calculated from the relation, $e_j^{(i)} = (M_j / M_i)\, e_i^{(j)} + 0.434 \times 10^{-2} (M_i - M_j / M_i)$

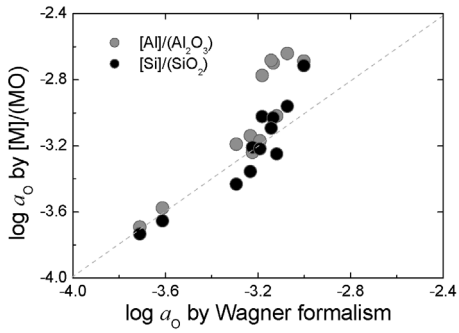

Figure 2: Relationship between the activities of oxygen calculated from the Wagner formalism, and the deoxidation equilibria by aluminum and silicon at 1873 K

are located in the *spinel+liquid* region, while those in equilibrium with the less basic (B < 1.7) slags are mostly in the *liquid* single phase. Here, the basicity of the slags, *B* is defined as follows.

$$B = (wt\%CaO + wt\%MgO)/(wt\%SiO_2 + wt\%Al_2O_3) \quad (10)$$

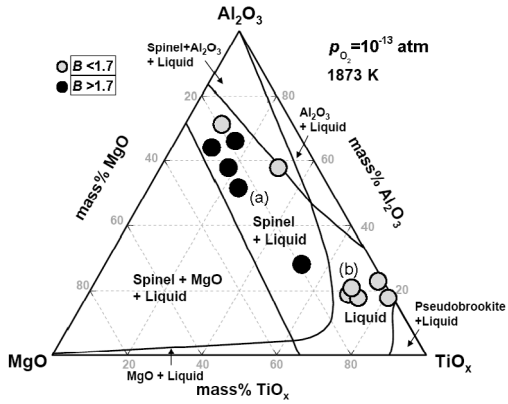

Figure 3: Computed phase diagram of the MgO-Al_2O_3-TiO_x system at 1873 K and $p_{O_2} = 10^{-13}$

However, in cases of relatively high concentration of Ti and Al, the composition of the inclusions was found to be in the *spinel+liquid* region, although the less basic slags are equilibrated. The thermodynamic effect of the slag composition on the inclusions will be discussed in detail later.

In order to quantitatively investigate the composition of the inclusions, the ratio of tri- and tetravalent titanium in liquid phase has also been calculated by FactSage™ 5.5 program and is shown in Figure 4 as a function of the (wt%MgO)/(wt%Al_2O_3) ratio. The ratio of (wt%Ti^{3+}) to (wt%Ti^{3+}+wt%Ti^{4+}) slightly increases by increasing the (wt%MgO)/(wt%Al_2O_3) ratio regardless of total content of titanium oxide. Nevertheless, it is considered from this calculation that the relative amount of Ti^{3+} would be more dominant than that of Ti^{4+} in the present MgO-Al_2O_3-TiO_x ternary system at 1873 K and $p_{O_2} = 10^{-13}$atm.

The effect of alumina activity in the slag on the content of alumina in the inclusions is shown in Figure 5 at 1873 K. The mole fraction of alumina in the inclusions, log $X_{Al_2O_3}$ linearly increases with increasing activity of alumina, log $a_{Al_2O_3}$ in the basic slags with the slope of 0.80 (r^2 =0.91),

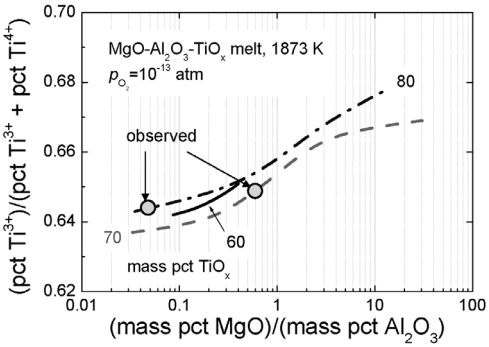

Figure 4: Computed ratio of (wt%Ti^{3+}) to (wt%Ti^{3+}+wt%Ti^{4+}) in the liquid phase of the MgO-Al_2O_3-TiO_x inclusion system at 1873 K and $p_{O_2} = 10^{-13}$atm.

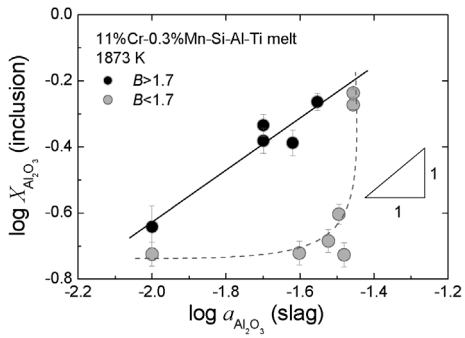

Figure 5: Relationship between the mole fraction of alumina in the inclusions and the activity of alumina in the slags at 1873 K in logarithmic scale

which is close to unity. This indicates that the activity coefficient of alumina in the inclusions would probably be constant when the basic (B > 1.7) slags are in equilibrium with the steel melts, whereas the stability of alumina in the inclusions could significantly be affected by the reaction between less basic (B < 1.7) but high alumina potential ($a_{Al_2O_3} > 0.03$) slags and the steel melts.

As shown in Figure 3, the composition of the inclusions could be grouped into the *spinel+liquid* and *liquid* oxides. Hence, the formation tendency of the spinel phase can qualitatively be estimated by considering the variation of the ratio of $(MgO)\times(Al_2O_3)$ to (Ti_2O_3) in the inclusions as the thermodynamic properties of the slag phase change. The relationship between the log $(X_{MgO} \times X_{Al_2O_3} / X_{Ti_2O_3})$ of the inclusions and the log $(a_{Al_2O_3} / a_{Ti_2O_3})$of the top slag at 1873 K is shown in Figure 6. The activity of TiO_2 was calculated by using FactSage™ 5.5 program.

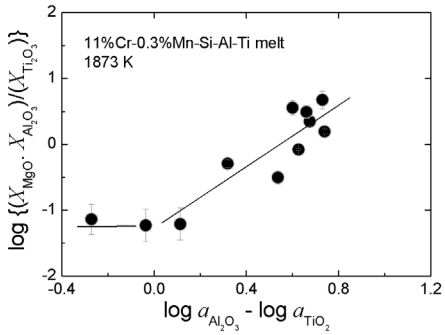

Figure 6: Effect of the log $(a_{Al_2O_3} / a_{Ti_2O_3})$of the slag on the log $(X_{MgO} \times X_{Al_2O_3} / X_{Ti_2O_3})$ of inclusions in the steel melts at 1873 K

It is of interest that the value of $(X_{MgO} \times X_{Al_2O_3} / X_{Ti_2O_3})$ is very low and nearly constant when the activity of Al_2O_3 is less than that of TiO_2 in the slag, followed by the linear increase with increasing log $(a_{Al_2O_3} / a_{Ti_2O_3})$. The activity of MgO in the slag could be fixed in the present study. Hence, the thermodynamic driving force for the formation of spinel-type inclusions is very low in the composition of $(a_{Al_2O_3} / a_{Ti_2O_3}) < 1$, while it linearly increases by increasing the activity ratio of Al_2O_3 to TiO_2 in the slag at $(a_{Al_2O_3} / a_{Ti_2O_3}) > 1$. This means that the activity of Al_2O_3 and TiO_2 in the slag significantly affects the formation behavior of the spinel-type inclusions in Ti-stabilized ferritic stainless steel melts, especially in case of MgO saturated slag and/or magnesia or dolomite refractory lining materials are used.

CONCLUSIONS

1. The activity of oxygen from [Al]/(Al_2O_3) and that from [Si]/(SiO_2) equilibria are relatively in good correspondence to each other with some scatters.

2. The composition of the inclusions could be plotted on the computed MgO-Al_2O_3-TiO_x phase diagram. The inclusions in the steel melts equilibrated with the basic slags are located in the *spinel + liquid* region, while those in equilibrium with the less basic slags are mostly in the *liquid* single phase. However, in cases of high concentration of Ti and Al, the inclusions were found to be *spinel + liquid*, although the less basic slags are equilibrated.

3. The log $(X_{MgO} \times X_{Al_2O_3} / X_{Ti_2O_3})$ is very low and nearly constant when the activity of Al_2O_3 is less than that of TiO_2 in the slag saturated by MgO, whereas it linearly increases by increasing the log $(a_{Al_2O_3} / a_{Ti_2O_3})$ at $(a_{Al_2O_3} / a_{Ti_2O_3}) > 1$.

REFERENCES

Gao, Y. & Sorimachi, K. (1993). *ISIJ International 33*, pp. 291-297. [1]

Maddalena, R., Rastogi, R., Bassem, S. & Cramb, A. W. (2000). *Iron & Steelmaker 27*, pp. 71-79. [2]

Nunnington, R. C. & Sutcliffe, N. (2001). *Electric Furnace Conf., Phoenix*, Nov. 11-14, pp. 361-394. [3]

Kim, J. W., Kim, S. K., Kim, D. S., Lee, Y. D. & Yang, P. K. (1996). *ISIJ International 36*, pp. S140-143. [4]

Kim, D. S., Park, J. H., Lee, S. B. & Lee, H. G. (2004). *Revue de Metallurgie 4*, pp. 291-299. [5]

Park., J. H. & Kim D. S. (2005.) *Metallurgical & Materials Transactions B 36B*, pp. 495-502. [6]

Okuyama, G., Yamaguchi, K., Takeuchi, S. & Sorimachi, K. (2000). *ISIJ International 40*, pp. 121-128. [7]

Park, J. H., Lee, S. B. & Gaye, H. R. (2008). *Metallurgical & Materials Transactions B 39B*, in press. [8]

Ohta, H., Suito H. (1998). *Metallurgical & Materials Transactions B 29B*, pp. 119-129. [9]

Gaye, H., Faral, M. & Lehmann, J. (2003). *Revue de Metallurgie 2*, pp. 125-134. [10]

http://www.factsage.com/ [11]

Kaufman, L. (1988). *Physica B+C 150*, pp. 99-114. [12]

Ruby-Meyer, F., Lehmann, J. & Gaye, H. (2000). *Scandinavian J. of Metallurgy 29*, pp. 206-212. [13]